



Thermodynamic analysis of a power cycle using a low-temperature source and a binary NH₃–H₂O mixture as working fluid

Philippe Roy^a, Martin Désilets^{b,*}, Nicolas Galanis^b, Hakim Nesreddine^c, Emmanuel Cayer^c

^aBBA 375, Boul. Sir Wilfrid-Laurier, Mont Saint-Hilaire (QC), Canada J3H 6C3

^bUniversité de Sherbrooke, département Génie mécanique, 2500 Boul. Université, Sherbrooke, Quebec, Canada J1K 2R1

^cLTE-Hydro-Québec, 600 av. de la Montagne, Shawinigan (QC), Canada G9N 7N5

ARTICLE INFO

Article history:

Received 9 September 2008

Received in revised form

14 May 2009

Accepted 26 May 2009

Available online 9 July 2009

Keywords:

Waste heat recovery

Energy analysis

Exergy analysis

Finite size thermodynamics

Heat exchanger surface

Optimization

ABSTRACT

Two Rankine cycles, one with and one without a regenerator, both using a NH₃–H₂O mixture as the working fluid, have been analyzed for fixed source and sink inlet temperatures. A fixed mass flow rate of a hot gaseous stream is providing the thermal energy input at the heat recovery boiler (HRB). The methodology used in this work is divided in four steps: energy analysis, exergy analysis, finite size (or finite time) thermodynamics (i.e. thermodynamic calculations in the context of reasonable temperature differences in the heat exchangers) and calculation of the heat exchangers' areas. The results show that the range of evaporation pressures satisfying some basic conditions increases with the source inlet temperature and with the ammonia concentration. They also show the existence of an optimum evaporation pressure for each of the four analyses. In the first two analyses, an optimum evaporation pressure of approximately 3.2 MPa maximises the thermal and exergetic efficiency, at respectively 11% and 73%. In the last two analyses, the optimum pressure of 2.5 MPa minimises the heat exchangers' areas. The results also show that the net power output generated from a limited energy source doesn't influence the results of the energy analysis. However, an increase of the net power output decreases the exergetic efficiency while at the same time it increases the heat exchangers' surface.

Crown Copyright © 2009 Published by Elsevier Masson SAS. All rights reserved.

1. Introduction

A large portion of the energy consumed by industries ends up as waste heat. A recent study [1] showed that the aluminium smelters in Canada produce 80 PJ of waste heat per year. If only 10% of this energy was recovered to produce useful work, Canadian aluminium producers could save up to 96 millions \$/year. This would also reduce the green house gas emissions by about 0.45 megatons/year. This is only one example illustrating the importance of recovering industrial waste heat.

A great deal of R&D effort has been devoted to find methods that can recover this waste heat and produce useful work. These methods are particularly interesting because they allow industries to become more energy efficient and to improve their productivity. For the past 20 year, extensive research has been carried out on the organic Rankine cycle (ORC) for the main purpose of converting low-temperature heat (80 °C < T < 300 °C) into electricity [2,3]. However, the thermal performance of such cycles is low if a pure

working fluid is used since such fluids have the property of boiling and condensing at constant temperatures. This leads to large temperature differences in the vapor generator and condenser which in turn increase entropy generation (i.e. irreversibility). To overcome this problem, other working fluids such as binary mixtures and supercritical fluids have been under investigation for the past 15 years [4–6]. The temperature of these fluids increases during heat addition. The resulting improved temperature matching between the two streams in the vapor generator reduces entropy generation as shown in Fig. 1, with the consequence of getting a higher specific work potential.

Cycles using a binary ammonia/water mixture as a working fluid offer interesting characteristics and a high potential for generating electricity from a low-temperature heat source. The first power cycle using such a mixture was proposed by Maloney and Robertson [7]. However, research on this concept was abandoned for approximately 25 years due to the rather poor performance results [7]. Later, Kalina [6] proposed another cycle using an ammonia/water mixture, which showed a 30–60% higher thermal efficiency than comparable steam power plant operating at a temperature of 560 °C. The first prototype of the Kalina cycle was constructed in 1991 [8]. Nowadays, the Kalina cycle has shown good performance

* Corresponding author. Tel.: +1 819 821 8000x63197; fax: +1 819 821 7163.
E-mail address: martin.desilets@usherbrooke.ca (M. Désilets).

Nomenclature

A	Area, m^2
C_p	Specific heat, $kJ/kg\cdot K$
D	Diameter, m
e	Specific exergy flow rate, kW/kg
\dot{E}	Exergy rate, kW
f	Darcy friction factor
g	Standard acceleration of gravity = $9.81 m/s^2$, m/s^2
h	Specific enthalpy, kJ/kg
i_g	Latent heat of evaporation, kJ/kg
k	Thermal conductivity, $kW/m\cdot K$
\dot{m}	Mass flow rate, kg/s
P	Pressure, Pa
Pr	Prandtl number
\dot{Q}	Heat transfer rate, kW
Re	Reynolds number
s	Specific entropy, $kJ/kg\cdot K$
T	Temperature, $^{\circ}C$ or K
U	Global convection heat transfer coefficient, $kW/m^2\cdot K$
UA	Overall thermal conductance, kW/K
w	Specific net power output, kW/kg
\dot{W}	Net power output, kW
x	Ammonia concentration

Greek symbols

α	Non-dimensional net power output
ε	Regenerator effectiveness
η	Efficiency
μ	Dynamic viscosity, $kg/m\cdot s$
ρ	Density, kg/m^3

Indices

c	condensation
d	destruction
e	evaporation
eq	equivalent
ex	exergetic
f	flow
fins	fins
g	waste heat gas source
is	isentropic
m	NH_3-H_2O mixture
o	dead state condition
p	pump
sat	saturation
t	turbine
w	cooling water sink

results in diverse applications, such as the first geothermal plant built in Husavik, Iceland [9]. Currently, the Kalina cycle has a great deal of interest in different applications [10]. Indeed, there are several different configurations of the Kalina cycle depending essentially on the heat source characteristics.

Despite the large number of published articles on the ORC and Kalina cycles [5,11,12], most are limited to first law (energy) and second-law (exergy) analyses. Very few authors have considered the finite size thermodynamic analysis [13,14]. None of them presented a rigorous analysis including variable heat transfer coefficient leading to the design and the calculation of the heat exchange areas. Furthermore, a constant C_p is assumed for the working fluid in the vast majority of the published results. This assumption can be questioned depending on the operating conditions. This aspect was studied in previous works [15,16].

The aim of the present article is to study the performance of two Rankine cycles using an ammonia/water mixture in order to convert a finite heat source such as waste heat from thermal

processes into electrical energy. The proposed methodology includes four different steps: energy analysis, exergy analysis, finite size thermodynamic analysis and calculation of all heat exchangers' areas. The numerical model takes into account some technical constraints, such as minimal vapour quality at the turbine exit, a constraint associated with typical equipments used in such systems. Turbine manufacturers usually recommend to keep the vapour quality over 90% to avoid erosion of the turbine blades. The variable properties of the ammonia/water mixture are also considered in the heat exchange calculation. Based on an elaborate review of the heat transfer coefficient in ammonia/water systems, the most recent correlations representing two-phase heat transfer are used in the design of major heat exchangers of the cycles studied. The proposed methodology was also followed for the study of a supercritical CO_2 cycle [17].

2. System description and modeling

The performance of two configurations is compared in this study, one with and the other without a regenerator (cf. Fig. 2). The cycle under study is identical to the traditional Rankine cycle. The working fluid is evaporated at a relatively high pressure, expands in a turbine and rejects heat in the condenser to water taken from a lake or a river whose temperature $T_{w,in}$ is specified. The condensate is then compressed in the pump and preheated in the regenerator if the temperature at state 2 is high enough. For this paper, the heat source considered is an industrial waste gas taken as air at a temperature of $100^{\circ}C$ with a mass flow rate of $314.5 kg/s$, figures representative of a real stream of industrial waste heat.

The following general assumptions are made in the thermodynamic analysis:

- Each component is considered as an open system in steady-state operation.
- The kinetic and potential energy changes are neglected.
- The heat and friction losses are also neglected.

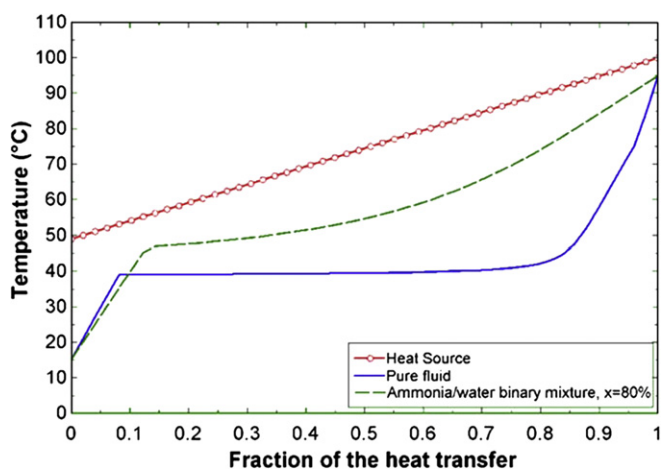


Fig. 1. Temperature variation in the HRB for pure fluid and for a NH_3-H_2O mixture.

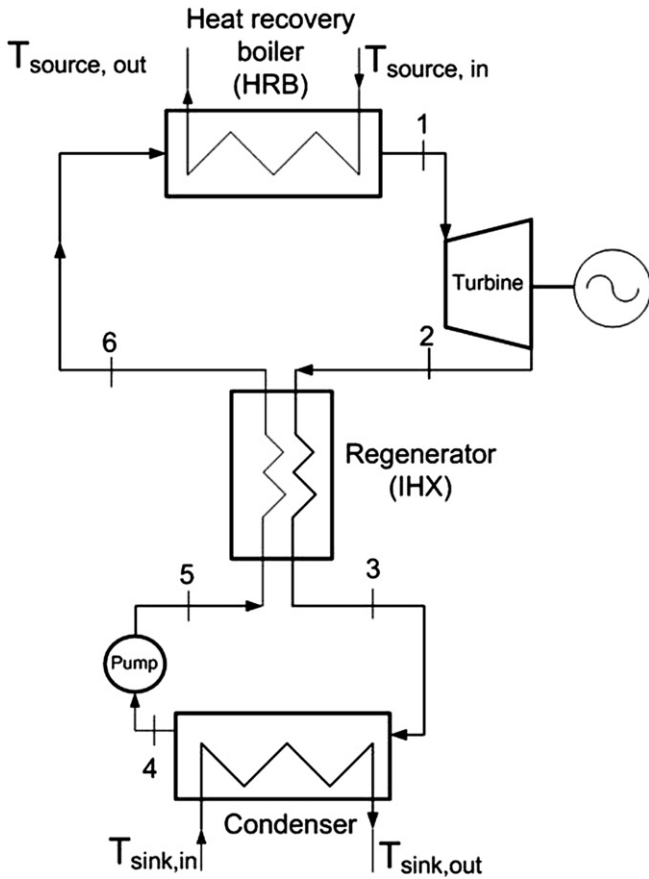


Fig. 2. Schematic representation of the system under study.

- The pump and the turbine isentropic efficiencies are 0.8 and the regenerator effectiveness is 0.5.
- The ammonia-water mixture at the condenser exit is a saturated liquid.
- The temperature $T_{g, in}$ is 100 °C and $T_{w, in}$ is 10 °C.
- A temperature difference of 5 °C is assumed between the working fluid and the external fluid for states 1 and 4, giving a maximum and a minimum cycle temperature of 95 °C and 15 °C respectively.
- All heat exchangers in the cycle (boiler, regenerator and condenser) (cf. Fig. 2) are considered as shell and tube counter-flow heat exchanger with one pass in the tubes and in the shell.

More detailed assumptions on the heat exchangers are made in Section 2.4.

The analysis is performed with EES (Engineering Equation Solver) [18]. This software has many advantages for thermodynamic analysis: the availability of fluid properties and of a solver for systems of non linear equations, to mention a few. The ammonia/water properties obtained with EES for several conditions have been compared with the ones in REFPROP [19], a package based on the data of the National Institute of Standards and Technology (NIST). The two sets of properties are essentially identical for all the conditions examined in this work.

2.1. Energy analysis

The equations presented here essentially express mass and energy balances for each component of the cycle. Taking into

consideration the assumptions already presented, the equations for the different components simplify to:

- for the pump:

$$\eta_{is,p} = \frac{v_4(P_e - P_c)}{h_5 - h_4} \quad (1)$$

$$\dot{W}_p = \dot{m}_m (h_5 - h_4) \quad (2)$$

- for the turbine :

$$\eta_{is,t} = \frac{h_1 - h_2}{h_1 - h_{2,is}} \quad (3)$$

$$\dot{W}_t = \dot{m}_m (h_1 - h_2) \quad (4)$$

- for the regenerator (IHX):

$$h_2 - h_3 = h_6 - h_5 \quad (5)$$

- for the heat recovery boiler (HRB):

$$\dot{Q}_{in} = \dot{m}_m (h_1 - h_6) \quad (6)$$

- for the condenser :

$$\dot{Q}_{out} = \dot{m}_m (h_3 - h_4) \quad (7)$$

The following two criteria of performance will be used to compare the two configurations of the ammonia/water Rankine cycle:

- specific net power output:

$$w = \frac{\dot{W}_t - \dot{W}_p}{\dot{m}_m} \quad (8)$$

- energy efficiency:

$$\eta = \frac{\dot{W}_t - \dot{W}_p}{\dot{Q}_{in}} \quad (9)$$

The regenerator efficiency is defined in terms of an enthalpy difference since a phase change at variable temperature may occur within this heat exchanger. Therefore, the usual simplification of constant specific heat is no longer valid. This is illustrated in Fig. 3 which shows the variation of specific heat with temperature at three different pressures. Consequently, the heat transfer process in the heat exchangers must be discretised and the properties must be evaluated at each point.

We chose to estimate the temperature at the low pressure outlet of the regenerator (state 3) by assuming an effectiveness for the regenerator:

$$T_3 = T_2 - \varepsilon(T_2 - T_5) \quad (10)$$

Where ε corresponds to the classical regenerator effectiveness based on the same constant specific heat for the high and low pressure fluids. As mentioned before the constant specific hypothesis is not valid in the present case. Nevertheless, equation 10 can be used in the model to determine a realistic value of T_3 ,

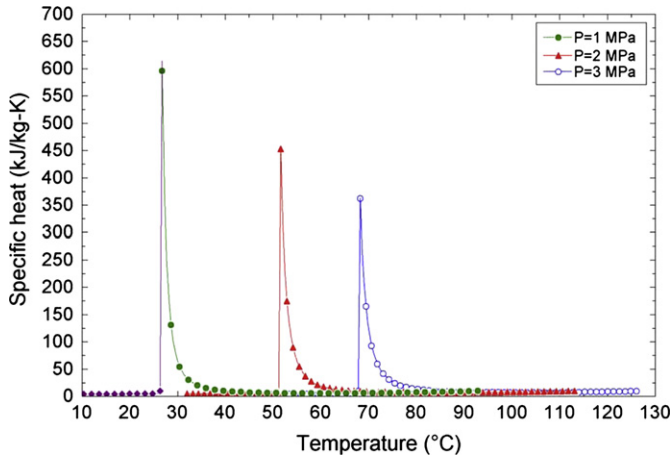


Fig. 3. Specific heat variation for a $\text{NH}_3\text{-H}_2\text{O}$ mixture ($x = 0.95$).

a starting point in our calculation process. Indeed for $0 > \varepsilon > 1$, the value of T_3 is always between T_2 and T_5 .

2.2. Exergy analysis

The objective behind the exergy analysis is to determine the operating conditions of a system which destroys the least available work. Such an analysis requires the mass flow rates of the system. Because of the limited heat source used in this study, a realistic assumption on the proportion of heat extracted by the power cycle is required. This is achieved by fixing the value of α , which represents the ratio between the net power generated by the system and the maximum power output corresponding to the specified characteristics of the source and sink. The latter is evaluated by considering a Carnot cycle operating between the inlet temperatures of the heat source and sink:

$$\dot{W}_{\max} = \dot{m}_g c_{p,g} (T_{g,\text{in}} - T_{w,\text{in}}) \left(1 - \frac{T_{w,\text{in}}}{T_{g,\text{in}}} \right) \quad (11)$$

Considering the limited waste heat source assumed, this maximum theoretical power is approximately 6.9 MW. With the specific net power output already known from the previous energy analysis, the mass flow rate of the ammonia/water binary mixture circulating in the cycle can then be determined from the following equation:

$$\dot{m}_m = \frac{\alpha \dot{W}_{\max}}{w} \quad (12)$$

An additional assumption is considered to evaluate the mass flow rate of the cooling water circulating in the condenser: the temperature rise of the cooling water is assumed to be 2°C . With this assumption, it is possible to calculate the mass flow rate of the water entering the condenser by the following equation:

$$\dot{Q}_{\text{out}} = \dot{m}_m (h_3 - h_4) = \dot{m}_w c_{p,w} (T_{w,\text{out}} - T_{w,\text{in}}) \quad (13)$$

Considering that the potential and kinetic energy have been neglected, the exergy of the $\text{NH}_3\text{-H}_2\text{O}$ mixture can be calculated from the following relation:

$$e = h - h_0 - T_0 (s - s_0) \quad (14)$$

Since the variations of the composition of the working fluid are limited to a few percent, the chemical exergy has been neglected. This assumption is also justified by the fact that only relative

changes in exergy are considered in this present work. Consequently, the dead state identified with the 0 subscript in the previous equation, has been defined as water at atmospheric pressure and 10°C .

The exergy destruction rate can then be calculated for each component of the cycle from the following exergy balance equation:

$$\dot{E}_d = \sum_i \dot{m}_{\text{in}} e_{\text{in}} - \sum_o \dot{m}_{\text{out}} e_{\text{out}} - \dot{W} \quad (15)$$

Finally, the previous exergy analysis makes it possible to calculate the exergy efficiency or second-law efficiency of the cycle from the following equation:

$$\eta_{\text{ex}} = 1 - \frac{\dot{E}_{d,\text{tot}}}{\dot{m}_g e_{g,\text{in}}} \quad (16)$$

2.3. Finite size thermodynamics analysis

The finite size thermodynamics analysis consists of characterising the heat transfer process in the cycle and evaluating the overall thermal conductance (UA) having assumed a reasonable temperature difference between the fluids in the heat exchangers. The coefficient UA (combination of the heat transfer surface and the overall heat transfer coefficient) must be determined for each heat exchanger by using methods such as LMTD or NTU- ε . However, these methods are based on constant properties and, therefore, lead to incorrect results in the case of ammonia/water mixtures, as previously mentioned. This problem can be overcome by dividing the heat exchangers into relatively small sections and by assuming constant properties in each section. The discretisation leads to dividing the overall enthalpy change for one of the streams into N equal enthalpy differences Δh . The enthalpy difference of the other stream is determined by an energy balance. With the known enthalpy difference and pressure, the corresponding temperatures and other thermodynamics properties at each intermediate state are determined. The heat exchanged in each discretisation step i and the fractional UA_i values are calculated from the following equations:

$$\dot{Q}_i = \dot{m}_{f1} (h_{f1,i+1} - h_{f1,i}) \quad (17a)$$

$$\dot{Q}_i = \dot{m}_{f2} (h_{f2,i+1} - h_{f2,i}) \quad (17b)$$

$$\dot{Q}_i = UA_i \frac{(T_{f2,i+1} - T_{f1,i+1}) - (T_{f2,i} - T_{f1,i})}{\ln \left\{ \frac{(T_{f2,i+1} - T_{f1,i+1})}{(T_{f2,i} - T_{f1,i})} \right\}} \quad (18a)$$

For the heat recovery boiler and the condenser, the discretisation is applied to the ammonia/water mixture. For the regenerator, it is applied to the mixture coming from the pump. Once the UA and A values are evaluated for each i section, the total A can be found by adding the contributions of all sections. Independence of the results with regards to discretisation has been verified. The numerical study showed that a discretisation of $N = 50$ is largely adequate.

When a sufficiently high enough number of steps is used, equation 19 can be simplified by replacing the logarithmic mean temperature difference (LMTD) by an arithmetic mean of the temperature differences along each discretisation step, without affecting the results.

$$\dot{Q}_i = UA_i \left(\frac{(T_{f2,i+1} - T_{f1,i+1})}{2} + \frac{(T_{f2,i} - T_{f1,i})}{2} \right) \quad (18b)$$

This simplification has beneficial effect on calculation time and numerical convergence. Fig. 4 shows the comparison between the classical LMTD method and the discretised approach proposed in this study for the calculation of UA at the HRB. It shows important differences between the results obtained with the two methods used to calculate the values of UA. Considering that the heat exchange involves a working fluid with variable properties, the discretisation method offers a more rigorous method and is thus chosen for the finite size thermodynamic analysis.

2.4. Calculation of the heat exchangers' surfaces

In order to complete the analysis, the heat exchangers' surfaces A_i must be evaluated. This analysis can be achieved by specifying the type and the geometric parameters of the chosen exchanger, and by evaluating the convection heat transfer coefficient for the two fluids. The overall heat transfer coefficient U can then be calculated and A is obtained from the previously determined value of UA. For the sake of simplicity, each heat exchanger is analysed by considering a counter-flow shell and tubes exchanger with one pass for all streams. Each heat exchanger (HRB, condenser, and regenerator) is modeled according to their specific characteristics described below.

2.4.1. Heat recovery boiler (HRB)

The HRB transfers heat from the waste heat gas to the binary ammonia/water mixture, a fluid that is undergoing phase change. According to the phases present, the HRB is actually divided in three distinctive sections which are the generator (liquid phase), the evaporator (mixture of liquid and gas) and the superheater (gas phase), as shown in Fig. 5.

The high pressure ammonia/water mixture flows inside the tubes while the waste heat gas is flowing in the shell. Due to the poor heat transfer coefficient between the waste heat gas and the tube walls, longitudinal fins are added on the outside of each tube. The number of tubes and the shell diameter are calculated from a mass balance by fixing:

- The minimum velocity V_{\min} for the liquid ammonia/water mixture at 0.8 m/s,
- The maximum velocity V_{\max} for the entering waste heat gas at 35 m/s.

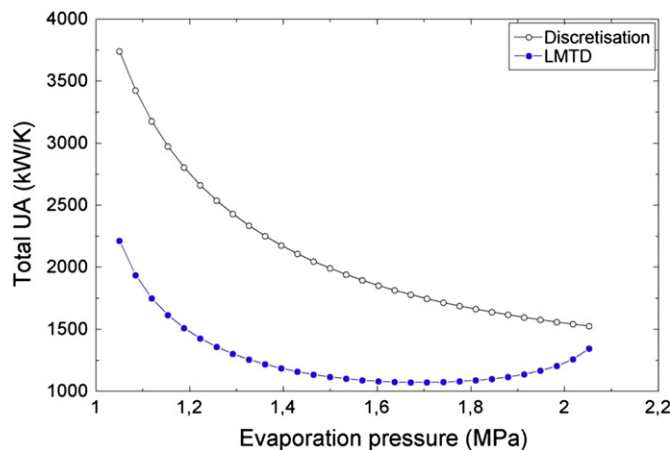


Fig. 4. LMTD vs discretisation approach.

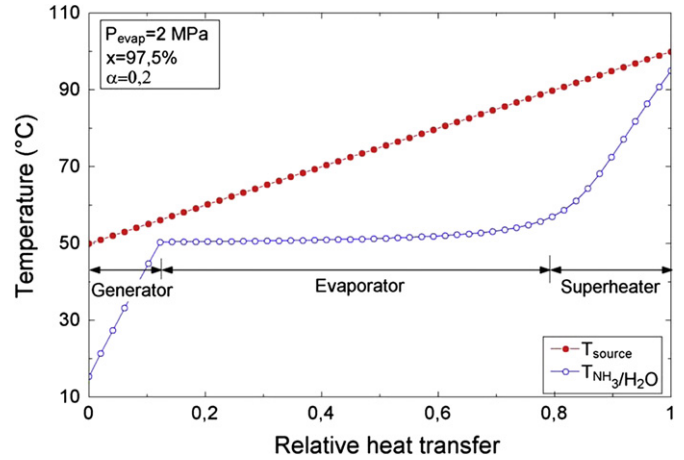


Fig. 5. Phases in the heat recovery boiler.

The V_{\min} on the mixture side is set to avoid fouling and to enhance heat transfer. The V_{\max} on the waste heat gas side is set to avoid excessive vibration.

As already mentioned, the HRB is discretised in 50 steps. The thermophysical properties such as the isobaric specific heat, the dynamic viscosity, the thermal conductivity and the density are evaluated with appropriate correlations for each step. There are numerous expressions that can be used to compute these thermophysical properties. The ones used in this study are based on the general review reported by Conde Engineering [20]. All properties are evaluated at the prevailing local conditions and are used to calculate the Prandtl and Reynolds numbers as well as the Darcy friction factor.

It is important to mention that these correlations depend on the phases present (liquid, mixture of liquid and vapour or vapour). For the waste heat gas and the ammonia/water mixture that do not undergo a phase change (single-phase), the Petukhov correlation [21] is applied. The choice of this correlation is based on the cylindrical geometry and on the fact that the working fluid studied is rich in ammonia, considered here as a pure fluid [22].

$$U_i = \frac{k_{g,i}}{D_{\text{eq}}} \left[\frac{\frac{f_{g,i}}{8} Re_{g,i} Pr_{g,i}}{12.7 \left(\frac{f_{g,i}}{8}\right)^{0.5} (Pr_{g,i}^{2/3} - 1) + 1.07} \right] \quad (19)$$

On the other hand, the heat transfer coefficient in the two-phase region is fixed to the reasonable value of $10 \text{ kW}/(\text{m}^2 \text{ K})$, based on the work of Stecco & Desideri [23]. Such a simple approach can easily be justified since this coefficient does not influence much the calculated value of the overall heat transfer coefficient. In fact, U depends mainly on the lowest heat transfer coefficient, found here on the waste heat gas side of the HRB. This approximation should have a negligible impact on the calculation of the HRB surface.

With the UA and heat transfer coefficients, the HRB surfaces on each side can be then calculated, using the following equation and the fins global efficiency:

$$\frac{1}{UA_i} = \frac{1}{\eta_{\text{fin},i} U_{g,i} A_{g,i}} + \frac{1}{U_{m,i} A_{m,i}} \quad (20)$$

The thermal resistance of the tube wall and fouling are neglected in this analysis.

2.4.2. Condenser

The numerical model of the condenser is similar to the HRB with few exceptions:

- The cooling water flows inside the tubes and the ammonia/water mixture in the shell.
- The number of tubes and shell diameter are estimated by the method described by Kakaç [24].
- The number of tubes and the shell diameter are calculated by assuming a minimum velocity of 2.8 m/s for the saturated liquid ammonia/water mixture.

The Petukhov's correlation (eq. 19) is employed on the cooling water side and for the single-phase ammonia/water mixture. For the two-phase region of the mixture, the Nusselt correlation for the condensation around a circular horizontal tube [24] is used:

$$U_{m,i} = 0.728 \left[\frac{\rho_{liq,i} (\rho_{liq,i} - \rho_{gas,i}) g i_{lg} D_{ext}^2}{\mu_{liq,i} (T_{sat} - T_{wall}) k_{liq,i}} \right]^{\frac{1}{4}} \left(\frac{k_{liq,i}}{D_{ext}} \right) \quad (21)$$

2.4.3. Regenerator (IHx)

The numerical model of the regenerator follows the same methodology used for the two previous heat exchangers. The high pressure mixture from the pump flows inside the tubes whereas the lower pressure mixture coming from the turbine flows inside the shell. Again, the fins are located outside the tubes to reduce the regenerator size. The number of tubes and the shell diameter are obtained by the same method used in the condenser. A minimum velocity of the saturated liquid ammonia/water mixture of 1.5 m/s is assumed in the IHx.

The Petukhov (eq. 19) and Nusselt (eq. 21) correlations are used for the low pressure ammonia/water mixture depending on the phase. For the ammonia/water mixture coming from the pump, the Petukhov's correlation (eq. 19) is used for the liquid phase while an approximate fixed value is used for the two-phase region, a region that is usually of minor importance.

3. Calculation methodology

As illustrated in Fig. 6, a global methodology including all described analyses has been developed. The numerical model is implemented in a single EES file.

The fixed and variables parameters must be established before any numerical analysis is conducted. In this study, the evaporation pressure, the non-dimensional net power output α and the ammonia concentration of the working fluid have been considered as the independent variables. The first study consists of an energy analysis of the cycle in which the net specific power output and the thermal efficiency are determined. Taking into account the source and the sink characteristics, a second-law analysis is then done. It consists of determining the mass flow rate of the working fluid, the exergy destruction in each components and the exergy efficiency of the cycle. Based on the energy and exergy analyses, the next step is to calculate the total UA coefficient having assumed counter-flow heat exchangers. Finally, considering specific geometric parameters like the fin characteristics and the maximum and minimum flow velocities in the exchangers, the overall heat transfer coefficient and the heat transfer area of each heat exchanger can be obtained. This procedure is repeated for a range of evaporation pressures in order to determine their influence on the performance of the cycle in terms of the specific net power output, the thermal and exergetic efficiency, and the total heat exchanger areas.

4. Results and discussion

In this section, the results of a parametric study for a NH₃-H₂O binary mixture Rankine cycle using the model previously described are presented. An introductory case is first analysed to highlight the main constraints associated with the application of this low-temperature cycle intended for the production of electrical energy from a finite industrial waste heat source.

4.1. Introductory case

In order to illustrate the limitations in terms of the evaporation pressure in this power cycle, the analysis will first be conducted with two selected ammonia/water mixtures having respectively an ammonia mass fraction of 0.975 and 0.99.

An upper bound on the evaporation pressure, P_{max} , can be determined by calculating the value of the evaporation pressure for which the liquid content of the mixture at the turbine exit becomes equal to 5%. A condensation of more than 5% of the vapour at the turbine outlet is deemed unacceptable since it could lead to erosion of the turbine blades. As expected for wetted fluids the quality at the turbine exit decreases when the evaporation pressure is increased.

As shown in Fig. 7, the vapour quality at state 2 is also a function of the ammonia concentration in the mixture. As the ammonia content is lowered, P_{max} decreases and the permitted pressure range tends to values for which such a cycle would not be practical. From Fig. 7, the ammonia concentration in the mixture must be over 95% ($x > 0.95$) to keep the liquid content below 5% at the turbine exit or equivalently to keep the quality of the vapour over 95%. In other words, the range of evaporation pressures that guarantees a quality superior to 95% at this location is quite restricted below $x = 0.95$. Results which are not presented here for lack of space indicate that this limiting effect is strongly influenced by the temperature at the turbine inlet.

Another important limitation comes from the specific net power output (or α). When α is increased, the admissible range of evaporation pressures is reduced in order to respect the pinch constraints at both ends of the HRB. In other words, the minimum evaporation pressure increases with α while the maximum evaporation pressure has to be reduced to avoid any temperature crossing in the boiler.

4.2. Energy analysis

In the first law analysis, results are reported for a unit mass flow rate of the working fluid. Therefore, the independent variables used in this section are the evaporation pressure P_e and the ammonia concentration x , since results are independent of the non-dimensional net power output α .

Fig. 8 shows the variation of the specific net power output and thermal efficiency as a function of the evaporation pressure, without the internal regenerator. For low evaporation pressure, w and η tend toward zero, as the evaporation pressure approaches the condensation pressure. The mixture having a lower ammonia concentration has a slightly higher w . However, since the range of P_e for lower ammonia concentration is more limited due to the quality constraint described in Section 4.1, a higher w is obtained with an ammonia concentration $x = 0.99$ at a maximum evaporation pressure of 3.22 MPa.

Analogously, Fig. 9 shows the variation of thermal efficiency and the specific net power output as a function of the evaporation pressure for the power cycle with an internal regenerator. In the present case, a maximum specific net power output of 150 kJ/kg is obtained at an evaporation pressure of 3.22 MPa, a value that is not affected

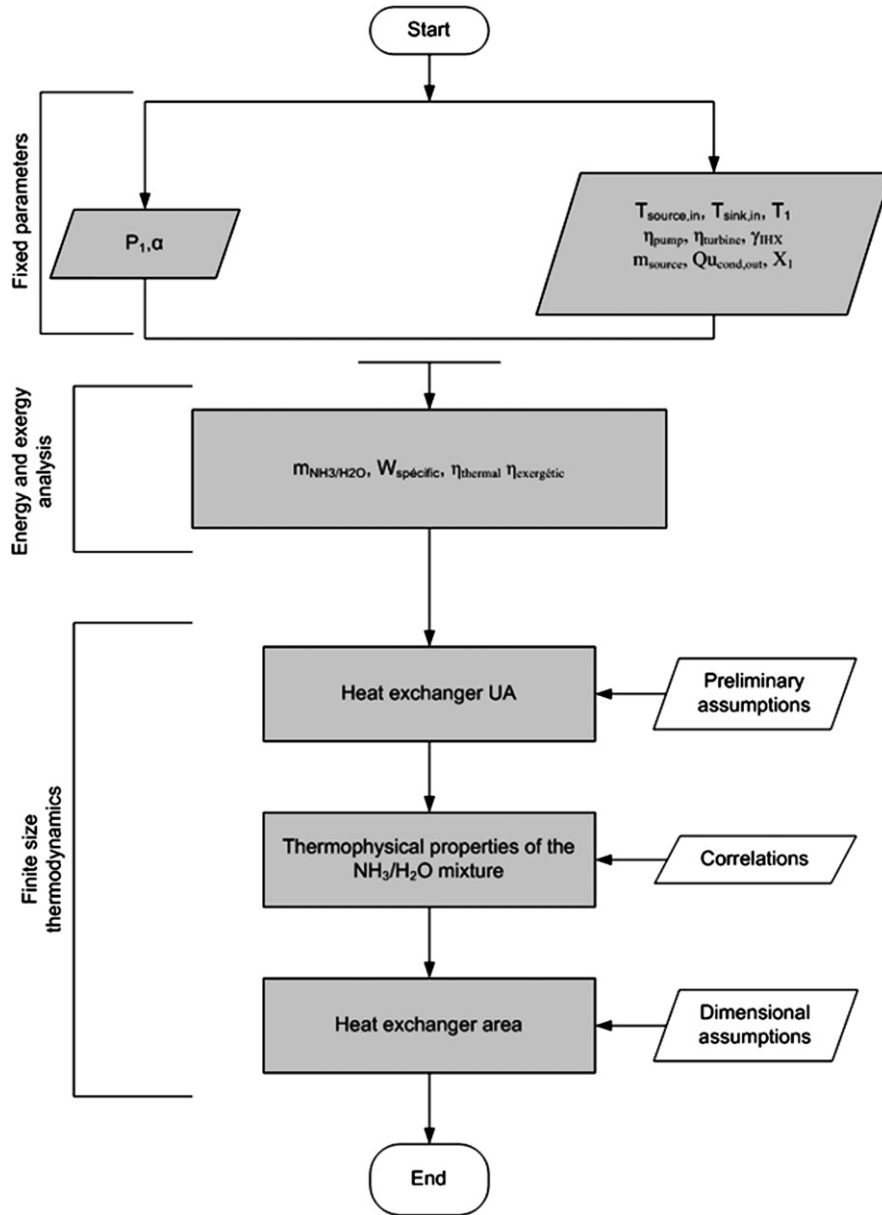


Fig. 6. Methodology.

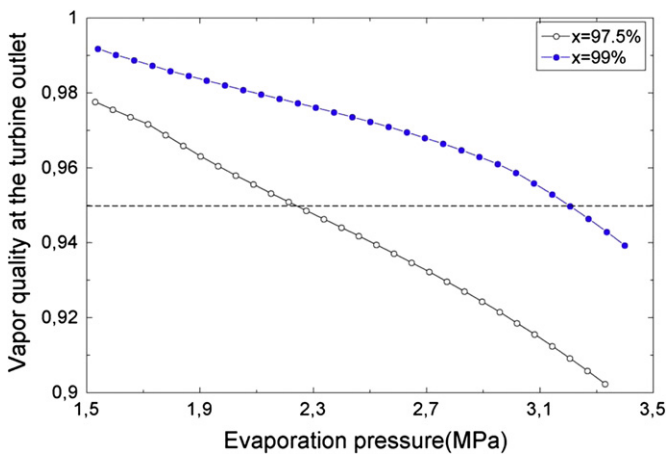


Fig. 7. Quality vs P_{max} for two ammonia concentrations.

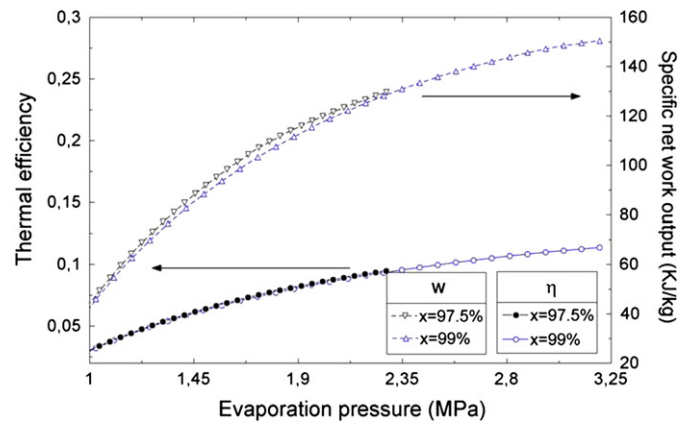


Fig. 8. Influence of ammonia concentration on thermal efficiency and net specific work.

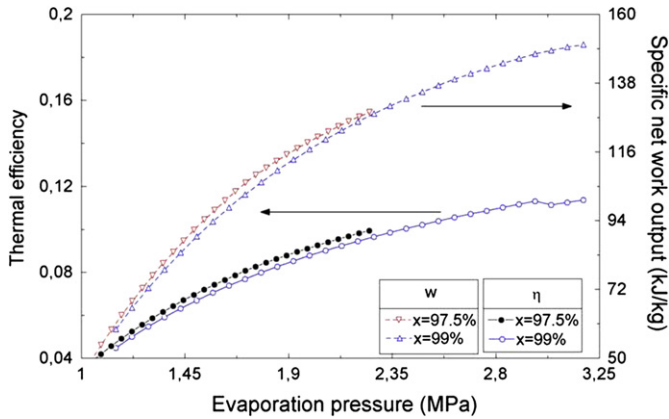


Fig. 9. Effect of regenerator on the thermal efficiency and the net specific work.

by presence of a regenerator. However, the maximum thermal efficiency is slightly influenced by the presence of the regenerator. The maximum thermal efficiency ($\eta = 11.39\%$) is obtained with the presence of a regenerator at an ammonia concentration of $x = 0.99$ and at an evaporation pressure of $P_e = 2.971$ MPa. The maximum thermal efficiency without the use of a regenerator ($\eta = 11.01\%$) is obtained at a higher evaporation pressure, $P_e = 3.22$ MPa.

The improvement brought by the regenerator is marginal (3% increase in thermal efficiency). Thus, it will probably be difficult to justify its use on an economical point of view. It is also interesting to note that such a component cannot be used for $P_e > 2.9$ MPa since at higher pressures, the temperature of the cold side of the regenerator exceeds that of the hot side.

4.3. Exergy analysis

As opposed to the previous energy analysis, the exergy analysis is influenced by the value of α or, equivalently, the net power output.

Fig. 10 shows the exergy efficiency of the Rankine cycle with regenerator for $\alpha = 0.2$ or, equivalently, a net power output of approximately 1.37 MW. The effect of the regenerator can be noticed up to an evaporation pressure of 2.9 MPa, on the curve of $x = 0.99$. These results indicate that for a fixed evaporation pressure, say 2 MPa, the mixture with a lower ammonia fraction ($x = 0.975$) has somewhat better exergy efficiency. This is due to a better matching of the temperature differences in both the HRB

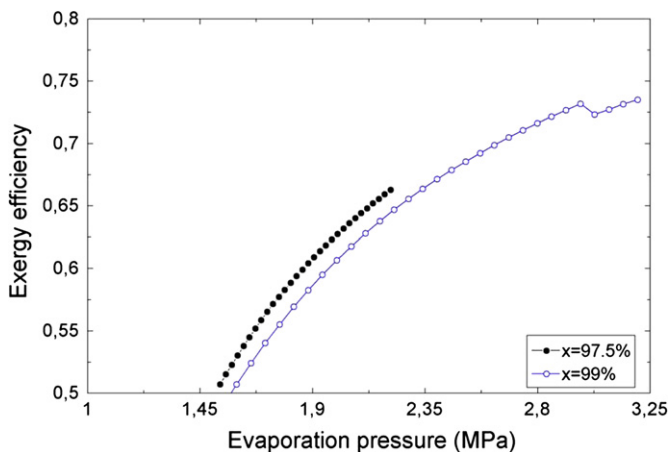


Fig. 10. Influence of ammonia concentration on exergetic efficiency ($\alpha = 20\%$).

and the condenser. However, since $\eta_{\text{exergetic}}$ increases with P_e and the range of allowable evaporation pressure is much larger for $x = 0.99$, the maximum value of the exergy efficiency is higher for the mixture with 99% ammonia. In fact, the maximum exergy efficiency is 73.2% for an evaporation pressure of 3 MPa and an ammonia concentration of $x = 0.99$.

The maximum exergy efficiency is essentially the same for the two configurations (with and without regenerator) under consideration. Based on the energy and exergy analyses, it can be concluded that the presence of the regenerator is hardly justifiable.

Fig. 11 illustrates the influence of α on the exergy efficiency as a function of the evaporation pressure for a system without a regenerator with an ammonia concentration of $x = 0.99$. From these results, it is evident that as α increases, the exergy efficiency decreases. In other words, when the net power output extracted from a fixed and limited heat source increases, the total exergy destruction also increases. This is due to the increase of the ammonia/water mixture mass flow rate which is proportional to net power output, α (cf eq. 12).

As already mentioned in Section 4.1, when α increases, the admissible range of evaporation pressure P_e is progressively reduced, down to a limiting value of α where only one evaporation pressure is permitted in order to respect the pinch constraints in the HRB. This effect can be clearly noticed from Fig. 11 where the admissible range of P_e is going from over 2.2 MPa at $\alpha = 10\%$ to approximately 1 MPa at $\alpha = 22\%$.

A specific exergy analysis for each component of this power cycle shows that roughly 45% of the destruction of exergy (irreversibility) is found in the HRB, 30% in the turbine, 10% in the pump and 15% in the condenser and the regenerator. The proportion of the irreversibility is slightly influenced by the evaporation pressure and α .

4.4. Finite size thermodynamics results

Fig. 12 shows a typical distribution of UA for a system with a regenerator operating with a mixture of 0.975 ammonia concentration and with $\alpha = 0.2$. The results show that the UA of the condenser largely dominates the other heat exchangers. This higher UA is explained by smaller temperature differences all along the exchanger.

Fig. 13 shows the influence of the ammonia concentration in the mixture on the UA of the whole system with a regenerator and with $\alpha = 0.2$. The results show that the mixture with an ammonia concentration of 0.975 has a slightly smaller minimum UA. This

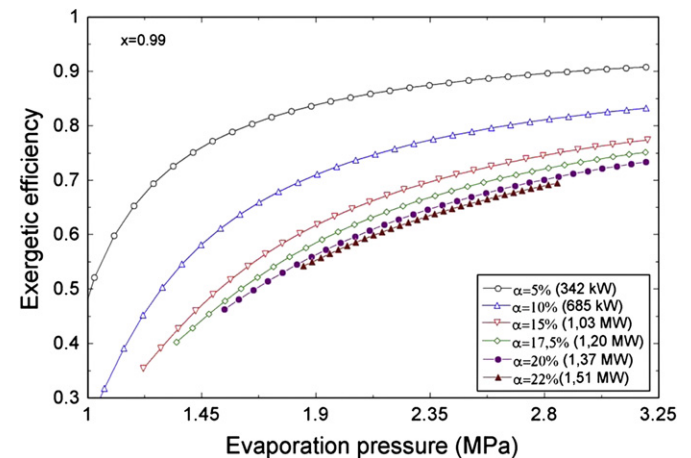


Fig. 11. Influence of α on exergetic efficiency.

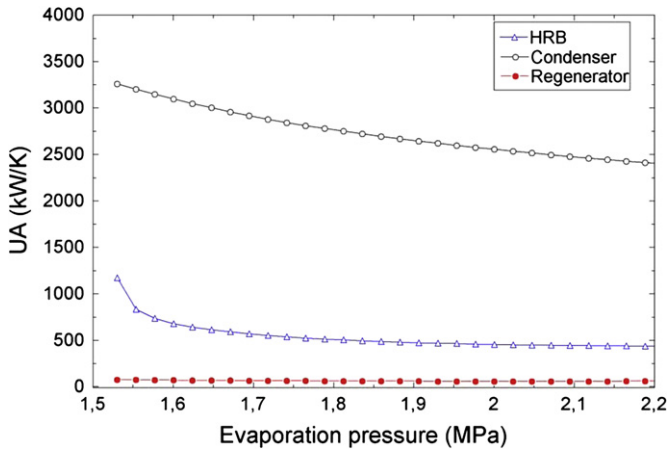


Fig. 12. Typical distribution of UA in the cycle ($x = 0.975$, $\alpha = 20\%$).

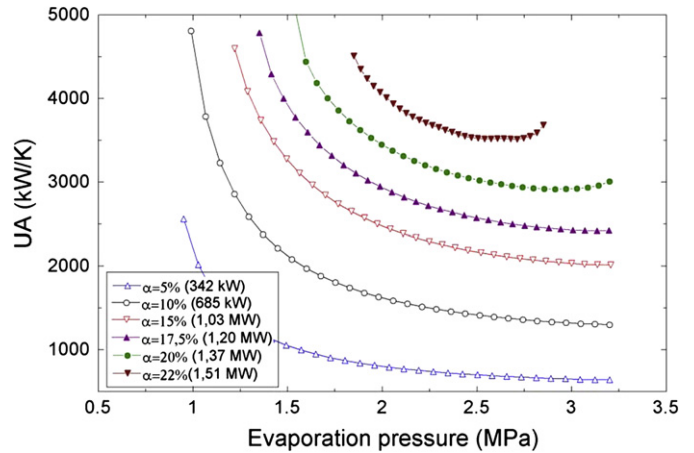


Fig. 14. Influence of α on UA, $x = 0.975$.

effect is due to a better thermal match of the temperature profiles in the HRB and the condenser. It is also important to point out that the minimum UA for $x = 0.975$ is obtained with a smaller evaporation pressure than for $x = 0.99$. It will probably result in smaller capital and operating costs.

To complete this section, Fig. 14 illustrates the influence of α on the total UA for a system without regenerator. The results show that total UA increases with α . Furthermore, each curve presents a noticeable minimum at an evaporation pressure which is essentially independent of α . The optimum evaporation pressure is approximately 2.5 MPa, slightly less than the one which maximises the thermal and exergetic efficiencies.

4.5. Heat exchange surface

Fig. 15 illustrates a typical distribution of the heat exchange area between the different heat exchangers of a Rankine cycle. It is based on the analysis of the configuration with a regenerator, operating with an ammonia concentration of $x = 0.99$ and for $\alpha = 0.2$. In opposition to the results obtained in the UA analysis (cf. Fig. 12), the HRB has the largest heat exchange surface because of the lower value of the heat transfer coefficient involved in this unit. Such results bring out the importance of this last analysis in the design and optimisation of the components of such a low-temperature power cycle.

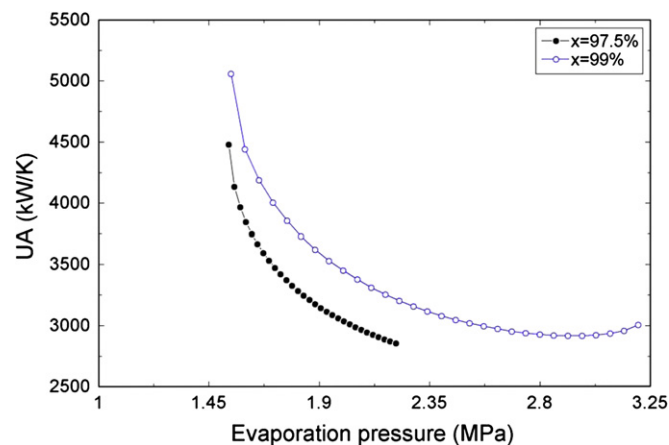


Fig. 13. Influence of ammonia concentration on UA ($\alpha = 20\%$, system with regenerator).

Fig. 16 shows the influence of the ammonia concentration on the total heat exchange area for a system with regenerator operating at $\alpha = 0.2$. The results show that a mixture with an ammonia concentration of $x = 0.975$ requires less total heat exchange surface than one with $x = 0.99$. These results also show that the minimum total heat transfer surface is 950 m^2 at an evaporation pressure of 2.3 MPa. The differences between the two curves can be explained by the better transport properties (thermal conductivity or viscosity) of the fluid richer in water. This in turn results in more efficient heat exchange thus smaller exchange area.

Similarly, Fig. 17 shows the influence of α on the total heat transfer surface for a system with a regenerator operating with an ammonia concentration of 0.99. The total heat exchange surface increases with α , each curve presenting a minimum at approximately $P_e = 2.4 \text{ MPa}$. The variation of α doesn't have a major impact on the optimizing evaporation pressure which lies between 2.2 and 2.6 MPa for a system operating with an ammonia concentration of $x = 0.99$.

Finally, Fig. 18 illustrates the network output of this low-temperature cycle obtained at the evaporation pressure that minimizes the total heat exchanger surface for two different concentrations of ammonia. The results show that for about the same value of \dot{W}_{net} , the mixture with $x = 0.975$ has a slightly lower heat exchanger surface compared to the mixture with $x = 0.99$, explained again by the higher transport properties of the lower ammonia mixture.

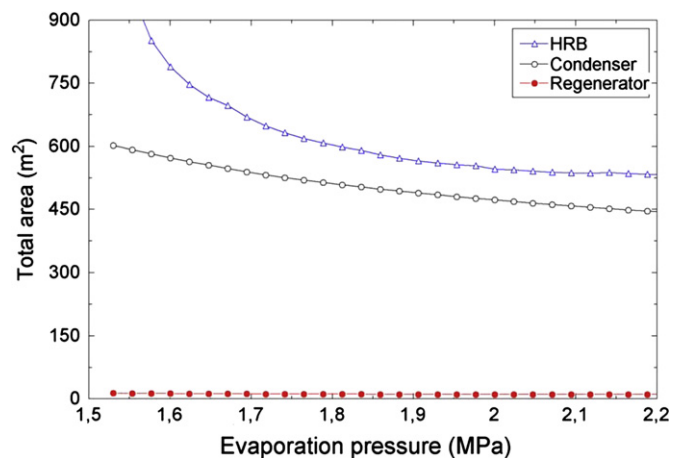


Fig. 15. Typical distribution of areas in the cycle ($x = 0.975$, $\alpha = 20\%$).

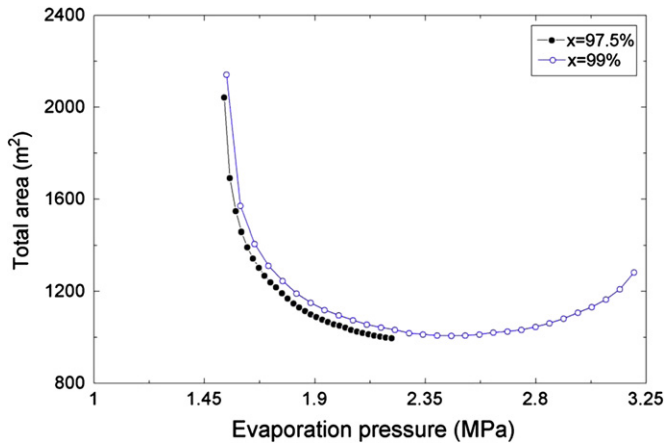


Fig. 16. Influence of ammonia concentration on heat exchange area ($\alpha = 20\%$).

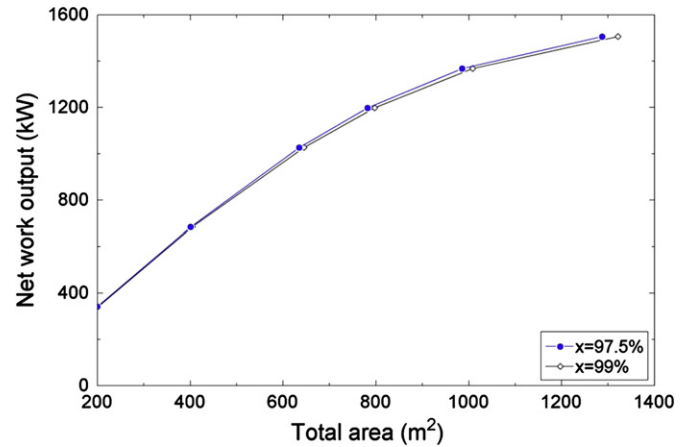


Fig. 18. Influence of x on minimum heat exchange area.

5. Conclusions

A four-step methodology was developed and used to study the performance of a $\text{NH}_3\text{-H}_2\text{O}$ binary mixture Rankine cycle with the following characteristics:

- heat source: temperature of 100°C , flow rate of 314.5 kg/s ,
- heat sink: cooling water at 10°C ,
- maximum and minimum temperatures of the $\text{NH}_3\text{-H}_2\text{O}$ binary working fluid: 95°C and 15°C respectively.

Three independent design variables have been considered: the evaporation pressure, the ammonia concentration and the net power output (or α), the values of which are constrained by some technical limitations related to a minimal quality of the vapour at the turbine exit. The following performance criteria have been used in the parametric study: the specific net work output, the thermal and exergetic efficiency, the overall thermal conductance and the total surface of the system's heat exchangers.

The principal findings are:

- ★ The proportion of heat extracted from the source (α) doesn't influence the energy analysis (specific net work output and thermal efficiency) but strongly affects the exergetic efficiency,

the overall UA coefficients and the total surface of the system's heat exchangers.

- ★ Unsurprisingly, the maximum thermal efficiencies of a Rankine cycle used to convert the energy contained in a waste heat gas at 100°C are low at approximately 11–12%, values obtained with at an ammonia concentration of $x = 0.99$ and P_e of 3.22 MPa .
- ★ The Rankine power cycle using an ammonia-water mixture as working fluid can operate with considerably high exergetic efficiencies even if the source considered is a low temperature, low exergy one. The maximum exergetic efficiency found in this study is 73.2% for an ammonia concentration of $x = 0.99$ and an evaporation pressure of 3 MPa .
- ★ Based on the thermodynamic analysis conducted, the presence of an internal regenerator is not justifiable with a limited heat source at 100°C . Even if a slightly positive impact can be noticed on the thermal and exergetic efficiency at lower pressures, the maxima are most of the time located at higher evaporation pressure, where the conditions are no longer adequate for the use of such equipment.
- ★ It is possible to find optimal operating conditions in terms of evaporation pressure. Both the UA — P_e and the A — P_e curves present an optimum at approximately 2.5 MPa .
- ★ The evaporation pressure that minimises the UA product also minimises the total surface of the heat exchangers; these pressures are slightly lower than the ones which are maximising the thermal and exergetic efficiencies.

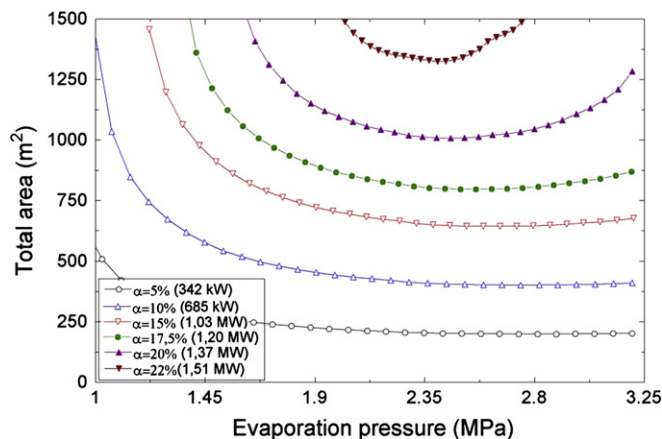


Fig. 17. Influence of α on area ($x = 0.99$).

For all results presented in this study, the quality of the vapour at the turbine exit was kept above 95% to avoid harmful condensation problems in the last stages of the turbine. In order to respect this constraint, the ammonia concentration was kept above $x = 0.975$. With a source at 100°C , the ammonia concentration of the mixture is thus limited to very high ammonia concentrations, $x = 0.975$ in this case.

Acknowledgements

This project is part of the R&D program of the NSERC Chair in Industrial Energy Efficiency established in 2006 at Université de Sherbrooke. The authors acknowledge the support of the Natural Sciences & Engineering Research Council of Canada, Hydro Québec, Rio Tinto Alcan and CANMET Energy Technology Center.

References

- [1] Market Study on Waste Heat and Requirements for Cooling and Refrigeration in Canadian Industry, Stricker Associates Inc, February 2006.
- [2] G. Angelino, C. Invernizzi, G. Molteni, The potential role of organic bottoming Rankine cycles in steam power stations, *Proceedings of the Institution of Mechanical Engineers – Part A* 213 (2) (1999) 75–81.
- [3] D. Wei, X. Lu, Z. Lu, J. Gu, Performance analysis and optimization of organic Rankine cycle (ORC) for waste heat recovery, *Energy Conversion and Management* 48 (4) (April 2007) 1113–1119.
- [4] T.-C. Hung, Waste heat recovery of organic Rankine cycle using dry fluids, *Energy Conversion and Management* 42 (2001) 539–553.
- [5] Y. Chen, P. Lundqvist, A. Johansson, P. Platell, A comparative study of the carbon dioxide transcritical power cycle compared with an organic Rankine cycle with R123 as working fluid in waste heat recovery, *Applied Thermal Engineering* 26 (17–18) (2006) 2142–2147.
- [6] A. Kalina, Combined cycle and waste heat recovery power systems based on a novel thermodynamic energy cycle utilizing low-temperature heat for power generation, *ASME-JPGC-GT* 83 (1983) 1–5.
- [7] O.M. Ibrahim, S.A. Klein, Absorption power cycles, *Energy* 21 (1) (1996) 21–27.
- [8] A. Kalina, Kalina cycles and system for direct-fired power plants, *Second Law Analysis – Industrial and Environmental Applications (ASME)* 25 (1991) 41–47.
- [9] H. Leibowitz, H. Micak, Design of a 2 MW cycle binary module for installation in Husavik, Iceland, *Geothermal Resources Council Transaction* 23 (1999) 17–20.
- [10] H.D. Madhawa, M. Golubovic, W. Worek, Y. Ikegami, The performance of the Kalina Cycle System (KCS-11) with low-temperature heat sources, *Journal of Energy Resources Technology (ASME)* 129 (2007) 243–247.
- [11] A. Kalina, Combined cycle system with novel bottoming cycle, *Journal of Engineering for Gas Turbine and Power* 106 (1984) 737–742.
- [12] C. Zamfirescu, I. Dincer, Thermodynamic analysis of a novel ammonia-water trilateral Rankine cycle, *Thermochimica Acta* 477 (2008) 7–15.
- [13] D. Stitou, M. Feidt, Nouveaux critères pour l'optimisation et la caractérisation des procédés thermiques de conversion énergétique, *International Journal of Thermal Sciences* 44 (2005) 1142–1153.
- [14] A. Bejan, Energy generation minimization: the new thermodynamics of finite-size devices and finite-time processes, *Journal of Applied Physics* 79 (3) (1996) 1191–1218.
- [15] E. Cayer, N. Galanis, M. Désilets and H. Nesreddine, First and second law analysis of an ammonia/water mixture Rankine cycle with low temperature heat sources, *Canadian Society for Mechanical Engineers Forum, Ottawa, Ont., Canada*, accepted, 2008.
- [16] P. Roy, N. Galanis, M. Désilets and H. Nesreddine, Étude Thermodynamique d'un Cycle Transcritique au Dioxyde de Carbone pour la Récupération de Chaleur de Basse Température, *Canadian Society for Mechanical Engineers Forum, Ottawa, Ont., Canada*, accepted, 2008.
- [17] E. Cayer, N. Galanis, M. Désilets, H. Nesreddine and P. Roy, Analysis of a carbon dioxide transcritical power cycle using a low temperature source, *Applied Energy* 86 (2009) 1055–1063.
- [18] F-Chart Software, Engineering Equation Solver (Commercial version).<https://www.fchart.com/> (2007) Web page.
- [19] Refprop Software (Commercial Version). NIST: standard reference; Version 7.0, 2002.
- [20] M. Conde Engineering, Thermo physical properties of NH₃/H₂O mixtures for the industries design of absorption refrigeration equipment, *Industrial report*, 2006.
- [21] F.P. Incropera, D.P. Dewitt, *Fundamentals of Heat and Mass Transfer*, Fifth ed, John Wiley & Sons, New York, 2002, p. 981.
- [22] E. Thorin, Thermophysical properties of ammonia-water mixtures for prediction of heat transfer areas in power cycles, *International Journal of Thermophysics* 22 (1) (2001).
- [23] S.S. Stecco, U. Desideri, Considerations on the design principles for a binary mixture heat recovery boiler, *Journal of Engineering for Gas Turbines and Power (Transactions of the ASME)* 114 (1992) 701–706.
- [24] S. Kakaç, H. Liu, *Heat Exchangers: Selection, Rating and Thermal Design*, Second ed, CRC Press, New York, 2002, p. 501.